Biogeosciences Discuss., 10, 18455–18478, 2013
www.biogeosciences-discuss.net/10/18455/2013/
doi:10.5194/bgd-10-18455-2013

Biogeosciences Discussions
Open Access

Spatial scale-dependent land-atmospheric methane exchange in the northern high latitudes from 1993 to 2004

X. Zhu[1], **Q. Zhuang**[1,2], **X. Lu**[3], **and L. Song**[1,4,5]

[1]Department of Earth, Atmospheric and Planetary Sciences, Purdue University, West Lafayette, IN 47907, USA
[2]Department of Agronomy, Purdue University, West Lafayette, IN 47907, USA
[3]The Ecosystems Center, Marine Biological Laboratory, Woods Hole, MA 02543, USA
[4]Institute of Geographic Sciences and Natural Resources Research, Chinese Academy of Sciences, Beijing, 100101, China
[5]Graduate University of the Chinese Academy of Sciences, Beijing, 100049, China

Received: 19 July 2013 – Accepted: 21 November 2013 – Published: 28 November 2013

Correspondence to: X. Zhu (zhu123@purdue.edu)

Published by Copernicus Publications on behalf of the European Geosciences Union.

Abstract

Effects of various spatial scales of water table dynamics on the land-atmospheric methane (CH_4) exchange have not yet been assessed for large regions. Here we used a coupled hydrology-biogeochemistry model to quantify daily CH_4 exchange over the pan-Arctic from 1993 to 2004 at two spatial scales (100 km and 5 km). The effects of sub-grid spatial variability of the water table depth (WTD) on CH_4 emissions were examined with a TOPMODEL-based parameterization scheme for northern high latitudes regions. Our results indicate that 5 km CH_4 emissions (38.1–55.4 Tg CH_4 yr^{-1}, considering the spatial heterogeneity of WTD) were 42 % larger than 100 km CH_4 emissions (using grid-cell-mean WTD) and the differences in annual CH_4 emissions were due to increased emitting area and enhanced flux density after WTD redistribution. Further, the inclusion of sub-grid WTD spatial heterogeneity also influences the inter-annual variability of CH_4 emissions. Soil temperature plays a more important role in the 100 km estimates, while the 5 km estimates are more influenced by WTD. This study suggests that previous macro-scale biogeochemical models using grid-cell-mean WTD might have underestimated the regional CH_4 budget. The spatial scale-dependent effects of WTD should be considered in future quantifications of regional CH_4 emissions.

1 Introduction

The importance of natural methane (CH_4) emissions from terrestrial ecosystems in the northern high latitudes in greenhouse gas radiative forcing has drawn a great attention in the past decades (e.g. Koven et al., 2011; Gao et al., 2013; Zhu et al., 2013a). The regional CH_4 budget and its temporal dynamics have been widely studied using "top-down" (e.g. Chen and Prinn, 2006; Kim et al., 2011) and "bottom-up" (e.g. Walter et al., 2001; Glagolev et al., 2011; Zhu et al., 2013b) approaches. However, it is still a challenge to have an accurate quantification given the high spatial and temporal variability of CH_4 emissions from this region (Solomon et al., 2007). Laboratory and field studies

BGD
10, 18455–18478, 2013

indicate that the dynamics of CH_4 fluxes are mainly determined by variations in water table, temperature, pH, and microbial substrate availability (Whalen and Reeburgh, 1996; MacDonald et al., 1998; Christensen et al., 2003; Wagner et al., 2005). As an effective "bottom-up" approach, process-based biogeochemical models are often used to study the effects of these environmental factors on CH_4 fluxes by considering the effects of soil hydrological and thermal dynamics on CH_4 production and consumption (e.g. Zhuang et al., 2004; Wania et al., 2010). Among these abiotic and biotic environmental controlling factors, the dynamics of the water table depth (WTD) is one of the most important factors in field observation (e.g. Nykänen et al., 1998; Heikkinen et al., 2002) and model-based (e.g. Petrescu et al., 2008; Bohn and Lettenmaier, 2010) studies.

Since the measurements of water table are only available at limited sites over the Earth's surface, most process-based biogeochemical models, operated at large grid cells (e.g. 0.5°), simply treat WTD as spatially uniform within each grid cell, without considering the sub-grid spatial heterogeneity of water table position (e.g. Walter et al., 2001; Zhuang et al., 2004, 2007). This simple representation of WTD may bias grid-cell-mean CH_4 fluxes, therefore regional CH_4 emissions. A recent model experiment that focused on a single model grid cell (100 km) (Bohn and Lettenmaier, 2010) indicated that the model-estimated CH_4 emissions without considering the sub-grid spatial heterogeneity of water table were biased by factors ranging from 0.5 to 2. Further, assuming different sub-grid spatial variability of WTD, simulated daily CH_4 fluxes were found to be biased low and high as the water table fell and rose, respectively. However, seasonal variability of WTD, which is greatly influenced by climate conditions, may obscure the impact of WTD on the bias of CH_4 emissions at a longer time scale. To date, it is still not clear how annual CH_4 budgets will be affected in their both direction and magnitude when the sub-grid spatial heterogeneity of WTD is taken into account.

To our knowledge, there is no such study on the effects of spatial scale-dependent WTD on CH_4 dynamics at large scales. Here we use a coupled hydrology-biogeochemistry model framework, incorporating sub-grid spatial variations in the WTD

BGD
10, 18455–18478, 2013

to assess CH_4 emissions from pan-Arctic terrestrial ecosystems with three objectives: (1) to quantify pan-Arctic land-atmospheric CH_4 exchanges at a fine spatial resolution by considering sub-grid spatial variability of WTD; (2) to analyze the spatial and temporal dynamics of CH_4 emissions; and (3) to examine the difference in the magnitude and temporal variability of CH_4 emissions with and without considering sub-grid spatial variability of WTD.

2 Methods

2.1 Overview

A macro-scale hydrological model (Variable Infiltration Capacity, VIC; Liang et al., 1994) and a biogeochemical model (Terrestrial Ecosystem Model, TEM; Zhuang et al., 2004) were coupled (Fig. 1) to make estimates of daily CH_4 exchange between terrestrial ecosystems and the atmosphere over the pan-Arctic, which is defined as the land area within the watersheds of major rivers that drain into the Arctic Ocean, excluding ice-dominated Greenland and Iceland (Lammers et al., 2001). To consider the effects of sub-grid spatial variability of WTD on estimated CH_4 emissions, the grid-cell-mean WTD simulated by VIC at a coarser spatial resolution was downscaled into a finer resolution at a sub-grid level using a TOPMODEL-based parameterization. The VIC-TEM-TOPMODEL framework was initially developed by Lu and Zhuang (2012) to estimate land-atmospheric CH_4 exchanges in the Alaskan Yukon basin. Here, the same coupled framework but with a new TOPMODEL-based parameterization scheme was used to assimilate satellite-based inundation data to improve the parameterization of TOPMODEL-based WTD redistribution.

2.2 Models and data

The TEM model explicitly simulates carbon and nitrogen dynamics of vegetation and soils, and has been used to examine terrestrial CH_4 dynamics in northern high latitudes

BGD
10, 18455–18478, 2013

(Zhuang et al., 2004; McGuire et al., 2010; Zhu et al., 2011). TEM has its hydrological module (Zhuang et al., 2002) to simulate water dynamics of terrestrial ecosystems. However, like many existing biogeochemistry models, the hydrological module is formulated as a simple "single-bucket". To improve the estimates of soil moisture profile, a key controlling factor for biogeochemical processes of CH_4, more sophisticated hydrological models, like VIC, are needed (e.g. Bohn and Lettenmaier, 2010; Lu and Zhuang, 2012). The VIC model used physically-based formulations to calculate energy fluxes and soil water movement and runoff (Liang et al., 1994). The explicit representation of the frozen soil/permafrost algorithm (Cherkauer et al., 2003) improved the capacity of the VIC model for cold region studies (Su et al., 2005, 2006). In the VIC-TEM-TOPMODEL framework (Fig. 1), the VIC model was first used to solve daily moisture and energy balances. The simulated soil temperature profile, freeze/thaw fronts, and soil ice profile were directly fed into TEM, while the simulated soil moisture profile was converted into WTD based on the soil moisture deficit method (Bohn et al., 2007) and then fed into TEM after redistributing WTD based on a TOPMODEL parameterization scheme. Finally, TEM was run to simulate daily CH_4 emissions and consumption over the pan-Arctic.

The process-based TEM model explicitly simulates CH_4 production, oxidation, and transport (diffusion, ebullition, and plant-aided transport) processes in the soil, with the following governing equation (Zhuang et al., 2004):

$$\frac{\partial C_M}{\partial t} = \frac{\partial (D(\partial C_M/\partial z))}{\partial z} + P - Q - E - R \ (\max(0, Z_{wt}) \le z \le Z_{soil}) \quad (1)$$

where ∂C_M is soil CH_4 concentration at a given depth (1 cm depth step) and a given time (1 h time step); $\partial(D(\partial C_M/\partial z))/\partial z$ is CH_4 diffusion and D is the CH_4 diffusivity in soil column; P, Q, E, and R represent the CH_4 production, oxidation, ebullition, and plant-aided transport rate, respectively; Z_{wt} is WTD and Z_{soil} is the lower boundary of the soil column. These CH_4-related processes were formulated as functions of climate, vegetation, and soil conditions for major terrestrial ecosystems in the northern high latitudes (Zhuang et al., 2004).

BGD
10, 18455–18478, 2013

To run the VIC and TEM models within the VIC-TEM-TOPMODEL framework, the spatial data of climate, vegetation, and soil from a variety of sources were used (Fig. 1). Gridded daily meteorological forcing data was acquired from NCEP/NCAR Reanalysis Datasets (http://www.esrl.noaa.gov/psd/data/gridded/data.ncep.reanalysis.surfaceflux.html). For VIC, precipitation, maximum/minimum air temperature and wind speed, were used. For TEM, precipitation, mean air temperature and downward solar shortwave radiation were required, except for those forcing from VIC simulations (soil temperature/moisture profiles and freezing/thawing fronts). For both VIC and TEM, gridded vegetation type information was derived from MODIS/MCD12C1 product with UMD vegetation classification scheme (https://lpdaac.usgs.gov/products/modis_products_table/mcd12c1), and gridded soil physical properties (e.g. soil texture, porosity) were taken from the World Inventory of Soil Emission Potentials (ISRIC-WISE) spatial soil database (Batjes, 2006). For the VIC model parameterization, vegetation-specific parameters (e.g. minimum stomatal resistance, rooting depths) were obtained from VIC model website (http://www.hydro.washington.edu/Lettenmaier/Models/VIC/), and typical calibration parameters that control soil water infiltration processes were taken from previous studies (Nijssen et al., 2001a, b, c). For the TEM model parameterization, key parameters that control methanogenesis and methanotrophy processes were taken from Zhuang et al. (2004).

2.3 TOPMODEL parameterization

In the VIC-TEM-TOPMODEL framework, the redistribution of WTD was made by applying topography-based watershed-scale TOPMODEL to represent spatial variability of local WTD. By assuming uniform soil hydraulic properties within each watershed and that local transmissivity decreases exponentially with depth (Beven and Kirkby, 1979), the relationship between local WTD (Z_{wt_i}) and watershed-mean water table ($\overline{Z_{\mathrm{wt}}}$) was expressed as:

$$Z_{\mathrm{wt}_i} = \overline{Z_{\mathrm{wt}}} - (\mathrm{TWI}_i - \overline{\mathrm{TWI}}) \times m \quad (2)$$

BGD
10, 18455–18478, 2013

where TWI_i represents local topographic wetness index, and $\overline{TWI}$ represents watershed-mean TWI. The watershed-mean water table ($\overline{Z_{wt}}$) was calculated as an area-weighted mean WTD of intersected VIC grid cells (Supplement Figs. S1 and S2). m is a decay parameter controlling the exponential decline of transmissivity with depth, and a larger m corresponds to deeper soil (slower declining rate of transmissivity with depth) and therefore stronger spatial variance of the local WTD (Z_{wt_i}) within a watershed. The magnitude of m is determined by the local sediment-bedrock profile, which is controlled by climate and geology/topography. Following Fan and Miguez-Macho (2011), the following equation was used to represent the effects of climate and topography on the parameter m over the pan-Arctic:

$$m = \frac{\alpha \times f_T}{1 + 150 \times s} \tag{3}$$

$$f_T = \begin{cases} 0.17 + 0.005 \times T & (T < -14^{\circ}C, f_T \geq 0.05) \\ 1.5 + 0.1 \times T & (-14^{\circ}C \leq T \leq -5^{\circ}C) \\ 1 & (T \geq -5^{\circ}C) \end{cases} \tag{4}$$

where s is local terrain slope; f_T is a temperature piecewise function used to represent the effect of frozen soil on soil drainage depth, in which T is mean surface air temperature in January; and α is a calibration parameter.

For each month of the period of 1993–2004, a three-step calibration procedure was used to best match the monthly TOPMODEL-based spatially-averaged fraction of inundated area to the monthly satellite-based inundation fraction over the pan-Arctic: (1) the spatially-averaged fraction of inundated area (A_i) in a month was first calculated from equal-area satellite-based inundation fraction data (Prigent et al., 2007; Papa et al., 2010); (2) the parameter α was calibrated to find an optimal value for that month to generate monthly Z_{wt_i} having a probability of $P(Z_{wt_i} \leq 0) = A_i$; and then (3) the optimal α was applied to each day in that month to calculate daily Z_{wt_i}. The daily Z_{wt_i} was set as zero whenever it was negative (above the soil surface) in the simulation of CH_4

BGD
10, 18455–18478, 2013

emissions. An illustration of TOPMODEL parameterization, description of topography-related spatial data, and calibration results were provided in the Supplement.

2.4 Simulation protocol

In this study, two sets of model simulations, with (referred to as VIC-TEM-TOPMODEL simulation) and without (referred to as VIC-TEM simulation) considering sub-grid spatial variability of WTD, were conducted to estimate daily CH_4 emissions. In the first set of simulations, we used the VIC-TEM-TOPMODEL framework to simulate daily CH_4 fluxes: VIC and TEM were operated at a spatial resolution of 100 km and 5 km, respectively, and the simulated 100 km grid-cell-mean WTD was redistributed into 5 km WTD at a sub-grid level via a TOPMODEL-based parameterization scheme. The choice of 5 km here was a special case of a finer spatial resolution for the VIC-TEM-TOPMODEL simulations, but the choice of any finer spatial resolution did not affect our simulations when the TOPMODEL-based parameterization scheme was applied. The probability distributions of 100 km and 5 km WTD over the region shared same mean value but with distinct variances. The variance of WTD increased after the redistribution of WTD, and the degree of the increase was determined by the parameter calibration (m in Eq. 2) with a target of best matching the simulated monthly inundated area fraction to the monthly satellite-based inundation fraction. Thus, the variance of WTD at a finer spatial resolution was only determined by satellite-based saturated area fraction; and the probability distribution of WTD at a finer scale did not change no matter what finer resolution was used. In the second set of simulations, only VIC and TEM models were used. In this case, both VIC and TEM were operated at the same spatial resolution (100 km) and no redistribution of WTD was applied. Due to the limited availability of satellite-based inundation data used for TOPMODEL-based parameterization scheme, these two sets of model simulations were run from 1993 to 2004. The VIC-TEM-TOPMODEL simulations at a 5 km spatial resolution were used to analyze the spatial and temporal dynamics of CH_4 emissions over the pan-Arctic. The effects of spatial scale-dependent WTD on CH_4 emissions were examined by comparing the

BGD
10, 18455–18478, 2013

100 km and 5 km CH_4 simulations with VIC-TEM-TOPMODEL and VIC-TEM models, respectively.

3 Results and discussion

3.1 Spatial patterns of methane fluxes

The VIC-TEM-TOPMODEL simulations indicated there is a large spatial variability of land-atmospheric CH_4 fluxes, simulated at a 5 km spatial resolution over the pan-Arctic (Fig. 2c). The highest emissions of CH_4 occurred in the West Siberian Lowlands (WSL, Fig. 2b) and the Hudson Bay Lowlands (HBL), where extensive wetlands exist, with a source of atmospheric CH_4 up to 400 mg CH_4 m^{-2} d^{-1} during the growing season (May–September). The sinks of atmospheric CH_4 occurred in the southern parts of Canada and Siberia, where drier ecosystems with higher soil temperatures favor CH_4 consumption, with a sink up to 1.5 mg CH_4 m^{-2} d^{-1}. Given the extremely high spatio-temporal variations of field CH_4 fluxes even under similar environmental conditions (e.g. Van Huissteden et al., 2005), a general evaluation of the magnitude and variability of simulated CH_4 fluxes was conducted here. In comparison with field CH_4 measurements, the estimated daily CH_4 fluxes during the growing season, $-1.5 \sim 400$ mg CH_4 m^{-2} d^{-1}, were within the range of reported CH_4 fluxes within the study region (Supplement Table S1), $-9 \sim 471$ mg CH_4 m^{-2} d^{-1}. The mean positive CH_4 flux (68.2 mg CH_4 m^{-2} d^{-1}), during the growing season, of all CH_4 emitting grid cells over the study region was closer to the mean value of site measurements of CH_4 emissions (60.1 mg CH_4 m^{-2} d^{-1}). In comparison with extensive field CH_4 measurements in WSL during the growing season ($\sim$ 1500 instantaneous measurements across representative mire landscapes) (Glagolev et al., 2011), the probability distributions of the modeled and observed daily CH_4 emissions had similar mean and median fluxes, although the model was unable to simulate extremely high CH_4 fluxes ($>$ 370 mg CH_4 m^{-2} d^{-1}) (Supplement Fig. S5).

BGD
10, 18455–18478, 2013

To analyze the relationship between 5 km CH_4 fluxes and major environmental controls, the WSL sub-region was further analyzed. The spatial patterns of CH_4 emissions and consumption were dominated by the distribution of WTD, although the spatial patterns were also affected by soil temperatures with a southward increasing trend (Fig. 2d and e). As expected, at a 5 km spatial resolution, shallower water table position corresponded to higher CH_4 emissions, while deeper water table position corresponded to lower CH_4 emissions and favored CH_4 consumption. In addition, positive CH_4 fluxes (i.e. net CH_4 emissions) generally occurred when the WTD was less than 0.5 m, beyond which soils generally acted as a sink of CH_4 (Fig. 2d and e).

Given the importance of water table in estimating CH_4 emissions, it was also worthwhile to evaluate the accuracy of the simulated WTD. The estimated WTD was compared with a dataset of water table observations, compiled by Fan et al. (2013). The comparison was limited to those well sites with shallow water table (< 2 m below the land surface) where soil moisture is coupled to water table (Fan et al., 2007), and around 5000 observations across southern Canada were available for the comparison (Supplement Fig. S7). Overall, the simulated WTD were comparable to the observations at well sites, although our estimates of water table were generally shallower as indicated by the histogram of WTD. The deeper water table at these well sites might be due to human activities including pumping, irrigation and drainage that were not represented in our model. In addition, the spatial pattern of WTD was generally consistent with an existing cartography-based 30-arc wetland map (GLWD-3, Lehner and Döll, 2004), although inconsistences existed in the southern part of the WSL (Fig. 2e and f). The depth of 0.5 m might have been used as a WTD threshold to determine the spatial distribution of wetlands in the WSL, although this WTD threshold was slightly deeper than those thresholds (0.2–0.4 m) suggested by Fan and Miguez-Macho (2011).

3.2 Temporal variability of methane fluxes

Driven with 12 yr climate data, 5 km CH_4 emissions from the VIC-TEM-TOPMODEL simulations showed that the inter-annual variability of CH_4 fluxes from terres-

BGD
10, 18455–18478, 2013

trial ecosystems over the pan-Arctic ranged from 38.1 Tg CH_4 yr^{-1} in 2000 to 55.4 Tg CH_4 yr^{-1} in 1994 (Fig. 3a). The estimated annual CH_4 emissions were within the range of previous measurements and model-based estimates, ranging from 20 to157 Tg CH_4 yr^{-1}, with the minimum and maximum values reported by Christensen et al. (1996) and Petrescu et al. (2010), respectively. There was a significant declining trend of annual net CH_4 emissions from 1993 to 2004, with an annual decreasing rate of 0.83 Tg CH_4 yr^{-2}. Correlation analysis indicated that annual 5 km CH_4 emissions were inversely correlated with WTD (statistically significant) and soil temperature (statistically insignificant), both of which had an increasing trend during the 12 yr period (Fig. 3a, Table 1). The high correlation coefficient ($r = -0.66$, at a significance level of $p < 0.05$) between annual 5 km CH_4 emissions and WTD highlights the importance of WTD in determining CH_4 fluxes.

To examine the seasonal variability of daily CH_4 emissions, we took the year 1994, having maximum 5 km CH_4 emissions from 1993 to 2004, as an example year for analysis (Fig. 3b). Most of emissions occurred from May to September, with the highest fluxes in July. Low CH_4 emissions were estimated in winter due to low soil temperature, while high CH_4 emissions occurred in summer due to high soil temperature and a shallow water table. Although both WTD and soil temperature influenced CH_4 emissions, the temporal dynamics of daily CH_4 fluxes are correlated better with WTD than soil temperature. Daily CH_4 emissions and WTD had a consistent seasonal variability with concurrent increases, peaks and decreases. The trough of CH_4 fluxes occurring in early August was caused by an abrupt drop-down of the water table, which could be attributed to the sudden decrease of precipitation but still high evapotranspiration (indicated by air temperature) in August (Supplement Fig. S6).

3.3 Differences due to spatial scales

There were large differences in both magnitude and temporal variability of methane emissions between 5 km VIC-TEM-TOPMODEL and 100 km VIC-TEM simulations.

BGD
10, 18455–18478, 2013

Mean annual net CH_4 emissions simulated at a 5 km resolution (45.8 Tg CH_4 yr^{-1}) from 1993 to 2004 were 42 % larger than those simulated at a 100 km resolution (32.2 Tg CH_4 yr^{-1}) (Fig. 3a). The 100 km CH_4 emissions tended to increase from 1993 to 2004 (statistically insignificant), which is contrary to the 5 km CH_4 emissions (Fig. 3a, Table 1). The inter-annual variability of the 100 km CH_4 emissions was positively correlated with soil temperature ($r = 0.84$, at a significance level of $p < 0.01$). Similarly, the 100 km daily CH_4 emissions had a consistent temporal variability with daily soil temperature (Fig. 3b). The 100 km CH_4 emissions were more dependent on soil temperature than on WTD. In contrast, WTD was more important in determining the 5 km CH_4 emissions.

The difference in the magnitude of annual net CH_4 emissions between 100 km and 5 km resolutions was due to changing emitting area and flux density. The fraction of CH_4 emitting area at a 5 km resolution was higher than that at a 100 km resolution due to the enhanced variance of 5 km WTD after WTD redistribution (19 % vs. 12 % over WSL, Fig. 4), although mean regional WTD was same. Mean flux density of 5 km resolution simulations over all emitting grid cells was larger than that of 100 km resolution due to the nonlinear dependence of CH_4 emissions on WTD (Fig. 4). The increases in both emitting area and CH_4 flux density resulted in a 42 % increase of annual net CH_4 emissions over the study region. The differences in CH_4 emissions at these two scales vary across the region and the annual total CH_4 budget over the study region at a 5 km resolution was consistently larger during the period of 1993–2004. Positive bias of CH_4 emissions (higher at a 5 km resolution) between the two scales tended to occur in those grid cells with deeper water table, while negative bias tended to occur in those with shallower water table (Fig. 5). This is consistent with the findings in Bohn and Lettenmaier (2010) that the simulated daily CH_4 fluxes without considering the sub-grid spatial heterogeneity of WTD (100 km simulation in our case) had biased high (low) under shallower (deeper) water table conditions.

In TEM, the emission rates of CH_4 have a positive temperature response and a negative WTD response (higher CH_4 emissions at shallower water table) (Zhuang et al.,

BGD
10, 18455–18478, 2013

2004). Our simulations show that WTD is influenced by temperature (deeper water table resulting from enhanced evapotranspiration at higher temperature), as indicated by the opposite inter-annual trends between water table and soil temperature (Fig. 3a). Thus, the relative importance of soil temperature and WTD on CH_4 emissions depends on their relative intensity and their interaction. According to the nonlinear dependence of CH_4 on WTD, the range of WTD can be conceptually divided into two emitting zones (Fig. 4): low-sensitivity zone (light-colored bars) and high-sensitivity zone (dark-colored bars). At a 100 km resolution (Fig. 4a), more emitting grid cells belonged to low-sensitivity zone, and thus the WTD had a relatively small influence on CH_4 emissions. On the contrary, at a 5 km resolution (Fig. 4b), more emitting grid cells belonged to high-sensitivity zone, and WTD became a dominant controlling factor (as shown in Fig. 2d and e).

4 Conclusions

Using a coupled hydrology-biogeochemistry model, two sets of simulations at two different spatial resolutions (100 km and 5 km) were conducted to explore the effects of sub-grid spatial variability of water table dynamics on CH_4 emissions over the pan-Arctic. The results suggest that previous macro-scale biogeochemical models using grid-cell-mean water table depth might have underestimated the regional CH_4 emissions. This study further indicate that spatial scale affects the quantification of the inter-annual variability of regional CH_4 emissions and the sub-grid spatial variability of water table depth should also be considered.

Supplementary material related to this article is available online at http://www.biogeosciences-discuss.net/10/18455/2013/bgd-10-18455-2013-supplement.pdf.

BGD
10, 18455–18478, 2013

Acknowledgement. The research is funded by a DOE SciDAC project and an Abrupt Climate Change project. This study is also supported through projects funded by the NASA Land Use and Land Cover Change program (NASA-NNX09AI26G), Department of Energy (DE-FG02-08ER64599), the NSF Division of Information and Intelligent Systems (NSF-1028291), and the NSF Carbon and Water in the Earth Program (NSF-0630319). This research is also in part supported by the Director, Office of Science, Office of Biological and Environmental Research of the US Department of Energy under Contract No. DE-AC02-05CH11231 as part of their Earth System Modeling Program.

References

Batjes, N. H.: ISRIC-WISE Derived Soil Properties on a 5 by 5 arc-minutes Global Grid (Version 1.0), ISRIC – World Soil Information, Wageningen, 2006.

Beven, K. J. and Kirkby, M. J.: A physically based, variable contributing area model of basin hydrology/Un modèle à base physique de zone d'appel variable de l'hydrologie du bassin versant, Hydrol. Sci. Bull., 24, 43–69, doi:10.1080/02626667909491834, 1979.

Bohn, T. J. and Lettenmaier, D. P.: Systematic biases in large-scale estimates of wetland methane emissions arising from water table formulations, Geophys. Res. Lett., 37, L22401, doi:10.1029/2010gl045450, 2010.

Bohn, T. J., Lettenmaier, D. P., Sathulur, K., Bowling, L. C., Podest, E., McDonald, K. C., and Friborg, T.: Methane emissions from western Siberian wetlands: heterogeneity and sensitivity to climate change, Environ. Res. Lett., 2, 045015, doi:10.1088/1748-9326/2/4/045015, 2007.

Chen, Y. H. and Prinn, R. G.: Estimation of atmospheric methane emissions between 1996 and 2001 using a three-dimensional global chemical transport model, J. Geophys. Res., 111, 1–25, 2006.

Cherkauer, K. A., Bowling, L. C., and Lettenmaier, D. P.: Variable infiltration capacity cold land process model updates, Global Planet. Change, 38, 151–159, 2003.

Christensen, T. R., Prentice, I. C., Kaplan, J., Haxeltine, A., and Sitch, S.: Methane flux from northern wetlands and tundra, Tellus B, 48, 652–661, 1996.

Christensen, T. R., Ekberg, A., Strom, L., Mastepanov, M., Panikov, N., Oquist, M., Svensson, B. H., Nykanen, H., Martikainen, P. J., and Oskarsson, H.: Factors controlling large

BGD
10, 18455–18478, 2013

scale variations in methane emissions from wetlands, Geophys. Res. Lett., 30, 1414, doi:10.1029/2002GL016848, 2003.
Fan, Y. and Miguez-Macho, G.: A simple hydrologic framework for simulating wetlands in climate and earth system models, Clim. Dynam., 37, 253–278, doi:10.1007/s00382-010-0829-8, 2011.
Fan, Y., Miguez-Macho, G., Weaver, C. P., Walko, R., and Robock, A.: Incorporating water table dynamics in climate modeling: 1. Water table observations and equilibrium water table simulations, J. Geophys. Res., 112, D10125, doi:10.1029/2006JD008111, 2007.
Fan, Y., Li, H., and Miguez-Macho, G.: Global Patterns of Groundwater Table Depth, Science, 339, 940–943, 2013.
Gao, X., Schlosser, C. A., Sokolov, A., Anthony, K. W., Zhuang, Q., and Kicklighter, D.: Permafrost degradation and methane: low risk of biogeochemical climate-warming feedback, Environ. Res. Lett., 8, 035014, doi:10.1088/1748-9326/8/3/035014, 2013.
Glagolev, M., Kleptsova, I., Filippov, I., Maksyutov, S., and Machida, T.: Regional methane emission from West Siberia mire landscapes, Environ. Res. Lett., 6, 045214, doi:10.1088/1748-9326/6/4/045214, 2011.
Heikkinen, J. E. P., Elsakov, V., and Martikainen, P. J.: Carbon dioxide and methane dynamics and annual carbon balance in tundra wetland in NE Europe, Russia, Global Biogeochem. Cy., 16, 1115, doi:10.1029/2002gb001930, 2002.
Kim, H. S., Maksyutov, S., Glagolev, M. V., Machida, T., Patra, P. K., Sudo, K., and Inoue, G.: Evaluation of methane emissions from West Siberian wetlands based on inverse modeling, Environ. Res. Lett., 6, 035201, doi:10.1088/1748-9326/6/3/035201, 2011.
Koven, C. D., Ringeval, B., Friedlingstein, P., Ciais, P., Cadule, P., Khvorostyanov, D., Krinner, G., and Tarnocai, C.: Permafrost carbon-climate feedbacks accelerate global warming, P. Natl. Acad. Sci. USA., 108, 14769–14774, 2011.
Lammers, R. B., Shiklomanov, A. I., Vörösmarty, C. J., Fekete, B. M., and Peterson, B. J.: Assessment of contemporary Arctic river runoff based on observational discharge records, J. Geophys. Res., 106, 3321–3334, doi:10.1029/2000JD900444, 2001.
Lehner, B. and Döll, P.: Development and validation of a global database of lakes, reservoirs and wetlands, J. Hydrol., 296, 1–22, doi:10.1016/j.jhydrol.2004.03.028, 2004.
Liang, X., Lettenmaier, D. P., Wood, E. F., and Burges, S. J.: A simple hydrologically based model of land surface water and energy fluxes for general circu-lation models, J. Geophys. Res., 99, 14415–14428, 1994.

BGD
10, 18455–18478, 2013

Lu, X. and Zhuang, Q.: Modeling methane emissions from the Alaskan Yukon River Basin, 1986–2005, by coupling a large-scale hydrological model and a process-based methane model, J. Geophys. Res., 117, G02010, doi:10.1029/2011jg001843, 2012.

MacDonald, J. A., Fowler, D., Hargreaves, K. J., Skiba, U., Leith, I. D., and Murray, M. B.: Methane emission rates from a northern wetland; response to temperature, water table and transport, Atmos. Environ., 32, 3219–3227, 1998.

McGuire, A. D., Hayes, D. J., Kicklighter, D. W., Manizza, M., Zhuang, Q., Chen, M., Follows, M. J., Gurney, K. R., McClelland, J. W., Melillo, J. M., Peterson, B. J., and Prinn, R. G.: An analysis of the carbon balance of the Arctic Basin from 1997 to 2006, Tellus B, 62, 455–474, doi:10.1111/j.1600-0889.2010.00497.x, 2010.

Nijssen, B., O'Donnell, G. M., Hamlet, A. F., and Lettenmaier, D. P.: Hydrologic sensitivity of global rivers to climate change, Climatic Change, 50, 143–175, 2001a.

Nijssen, B., O'Donnell, G. M., Lettenmaier, D. P., Lohmann, D., and Wood, E. F.: Predicting the discharge of global rivers, J. Climate, 14, 3307–3323, 2001b.

Nijssen, B., Schnur, R., and Lettenmaier, D. P.: Global retrospective estimation of soil moisture using the Variable Infiltration Capacity Land Surface Model, 1980–93, J. Climate, 14, 1790–1808, 2001c.

Nykänen, H., Alm, J., Silvola, J., Tolonen, K., and Martikainen, P. J.: Methane fluxes on boreal peatlands of different fertility and the effect of long-term experimental lowering of the water table on flux rates, Global Biogeochem. Cy., 12, 53–69, 1998.

Papa, F., Prigent, C., Aires, F., Jimenez, C., Rossow, W. B., and Matthews, E.: Interannual variability of surface water extent at the global scale, 1993–2004, J. Geophys. Res., 115, D12111, doi:10.1029/2009JD012674, 2010.

Petrescu, A. M. R., van Huissteden, J., Jackowicz-Korczynski, M., Yurova, A., Christensen, T. R., Crill, P. M., Bäckstrand, K., and Maximov, T. C.: Modelling CH_4 emissions from arctic wetlands: effects of hydrological parameterization, Biogeosciences, 5, 111–121, doi:10.5194/bg-5-111-2008, 2008.

Petrescu, A. M. R., van Beek, L. P. H., van Huissteden, J., Prigent, C., Sachs, T., Corradi, C. A. R., Parmentier, F. J. W., and Dolman, A. J.: Modeling regional to global CH_4 emissions of boreal and arctic wetlands, Global Biogeochem. Cy., 24, GB4009, doi:10.1029/2009gb003610, 2010.

BGD
10, 18455–18478, 2013

Prigent, C., Papa, F., Aires, F., Rossow, W. B., and Matthews, E.: Global inundation dynamics inferred from multiple satellite observations, 1993–2000, J. Geophys. Res., 112, D12107, doi:10.1029/2006JD007847, 2007.

Solomon, S., Qin, D., Manning, M., Chen, Z., Marquis, M., Averyt, K. B., Tignor, M., and Miller, H. L.: Climate Change 2007: The Physical Science Basis: Working Group I Contribution to the Fourth Assessment Report of the IPCC, Cambridge University Press, Cambridge, UK and New York, NY, USA, 2007.

Su, F., Adam, J. C., Bowling, L. C., and Lettenmaier, D. P.: Streamflow simulations of the terrestrial Arctic domain, J. Geophys. Res., 110, D08112, doi:10.1029/2004JD005518, 2005.

Su, F., Adam, J. C., Trenberth, K. E., and Lettenmaier, D. P.: Evaluation of surface water fluxes of the pan-Arctic land region with a land surface model and ERA-40 reanalysis, J. Geophys. Res., 111, D05110, doi:10.1029/2005JD006387, 2006.

Van Huissteden, J., Maximov, T. C., and Dolman, A. J.: High methane flux from an arctic floodplain (Indigirka lowlands, eastern Siberia), J. Geophys. Res., 110, G02002, doi:10.1029/2005JG000010, 2005.

Wagner, D., Lipski, A., Embacher, A., and Gattinger, A.: Methane fluxes in permafrost habitats of the Lena Delta: effects of microbial community structure and organic matter quality, Environ. Microbiol., 7, 1582–1592, 2005.

Walter, B. P., Heimann, M., and Matthews, E.: Modeling modern methane emissions from natural wetlands 1. Model description and results, J. Geophys. Res., 106, 34189–34134, 2001.

Wania, R., Ross, I., and Prentice, I. C.: Implementation and evaluation of a new methane model within a dynamic global vegetation model: LPJ-WHyMe v1.3.1, Geosci. Model Dev., 3, 565–584, doi:10.5194/gmd-3-565-2010, 2010.

Whalen, S. C. and Reeburgh, W. S.: Moisture and temperature sensitivity of CH_4 oxidation in boreal soils, Soil Biol. Biochem., 28, 1271–1281, 1996.

Zhu, X., Zhuang, Q., Chen, M., Sirin, A., Melillo, J., Kicklighter, D., Sokolov, A., and Song, L.: Rising methane emissions in response to climate change in Northern Eurasia during the 21st century, Environ. Res. Lett., 6, 045211, doi:10.1088/1748-9326/6/4/045211, 2011.

Zhu, X., Zhuang, Q., Gao, X., Sokolov, A., and Schlosser, C. A.: Pan-Arctic land–atmospheric fluxes of methane and carbon dioxide in response to climate change over the 21st century, Environ. Res. Lett., 8, 045003, doi:10.1088/1748-9326/8/4/045003, 2013a.

BGD
10, 18455–18478, 2013

Zhu, X., Zhuang, Q., Qin, Z., Glagolev, M., and Song, L.: Estimating wetland methane emissions from the northern high latitudes from 1990 to 2009 using artificial neural networks, Global Biogeochem. Cy., 27, 592–604, doi:10.1002/gbc.20052, 2013b.

Zhuang, Q., McGuire, A. D., O'Neill, K. P., Harden, J. W., Romanovsky, V. E., and Yarie, J.: Modeling soil thermal and carbon dynamics of a fire chronosequence in interior Alaska, J. Geophys. Res., 107, 8147, doi:10.1029/2001jd001244, 2002.

Zhuang, Q., Melillo, J. M., Kicklighter, D. W., Prinn, R. G., McGuire, A. D., Steudler, P. A., Felzer, B. S., and Hu, S.: Methane fluxes between terrestrial ecosystems and the atmosphere at northern high latitudes during the past century: a retrospective analysis with a process-based biogeochemistry model, Global Biogeochem. Cy., 18, GB3010, doi:10.1029/2004gb002239, 2004.

Zhuang, Q., Melillo, J. M., McGuire, A. D., Kicklighter, D. W., Prinn, R. G., Steudler, P. A., Felzer, B. S., and Hu, S.: Net emissions of CH_4 and CO_2 in Alaska: implications for the region's greenhouse gas budget, Ecol. Appl., 17, 203–212, 2007.

BGD
10, 18455–18478, 2013

Table 1. Pearson correlations between annual CH_4 emissions (at 5 km and 100 km resolutions) and spatially-averaged water table depth and top-layer (0–5 cm) soil temperature during the growing season (May–September) over the pan-Arctic during the period of 1993–2004. The annual changing rate of each variable is given in corresponding bracket.

	Water table depth ($0.2\,cm\,yr^{-1}$)	Soil temperature ($0.046^{a}\,°C\,yr^{-1}$)
CH_4 emissions at a 5 km resolution ($-0.83^{a}\,Tg\,CH_4\,yr^{-2}$)	-0.66^{a}	−0.36
CH_4 emissions at a 100 km resolution ($0.74\,Tg\,CH_4\,yr^{-2}$)	−0.15	0.84^{b}

[a] p value less than 0.05.
[b] p value less than 0.01.

BGD
10, 18455–18478, 2013

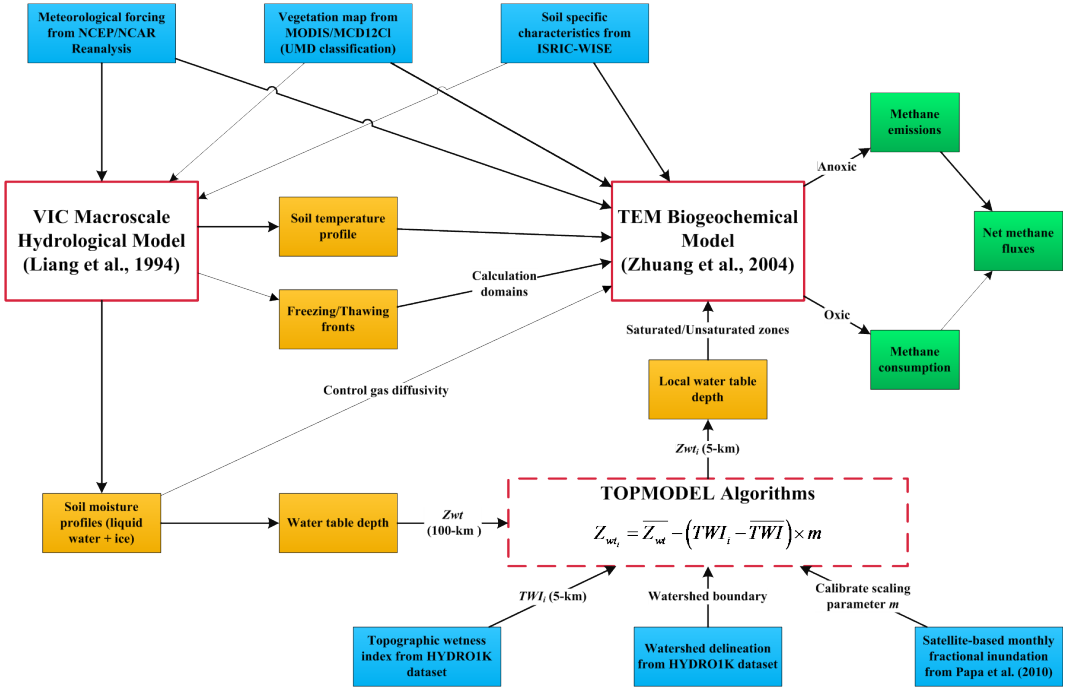

Fig. 1. Conceptual framework of coupled models to estimate net methane emissions. Shown are external spatial inputs (blue) for driving or calibrating models, internal information exchange (yellow) between models, and final model outputs (green). Arrows indicate the direction of information exchange among all components. See text and auxiliary materials for more details.

BGD
10, 18455–18478, 2013

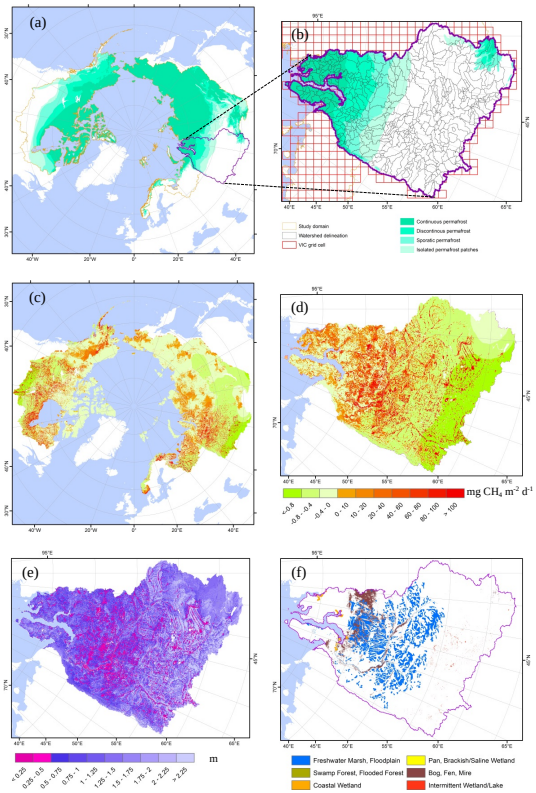

Fig. 2. The study domain, the pan-Arctic, overlaid with the distribution of permafrost **(a)**, example sub-region (West Siberian Lowlands) with watershed delineation and VIC grid cells **(b)**, mean daily methane fluxes (**c** and **d**) and water table depth **(e)** during the growing season (May–September) at a 5 km spatial resolution, and cartography-based GLWD wetland data **(f)** (Lehner and Döll, 2004).

BGD
10, 18455–18478, 2013

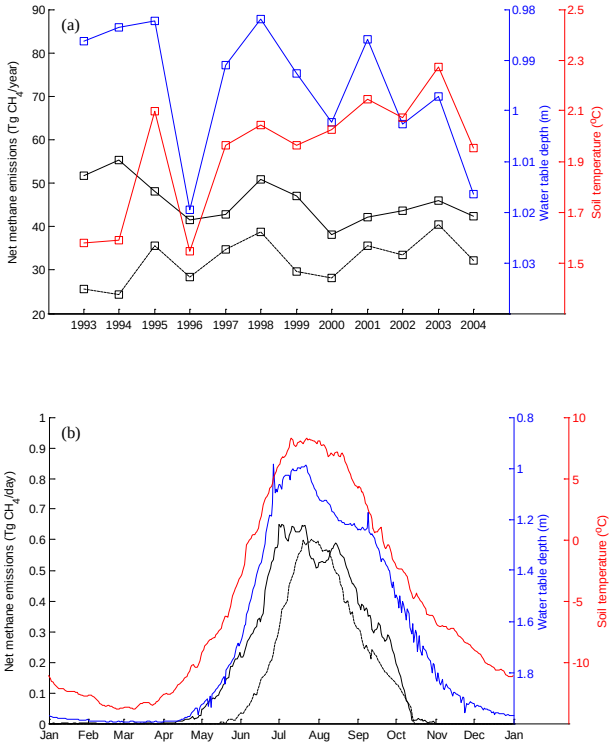

Fig. 3. Inter-annual **(a)** and seasonal **(b)** variability of simulated 5 km net methane emissions over the pan-Arctic and spatially-averaged water table depth and top-layer (0–5 cm) soil temperature. Mean water table depth and soil temperature during the growing season (May–September) are shown for inter-annual variability, and dashed lines represent simulated methane emissions at a 100 km spatial resolution. The daily simulations of year 1994, having maximum annual methane emissions at a 5 km resolution, are shown for the seasonal variability. Note the water table depth has an inverse y-axis different from others.

BGD
10, 18455–18478, 2013

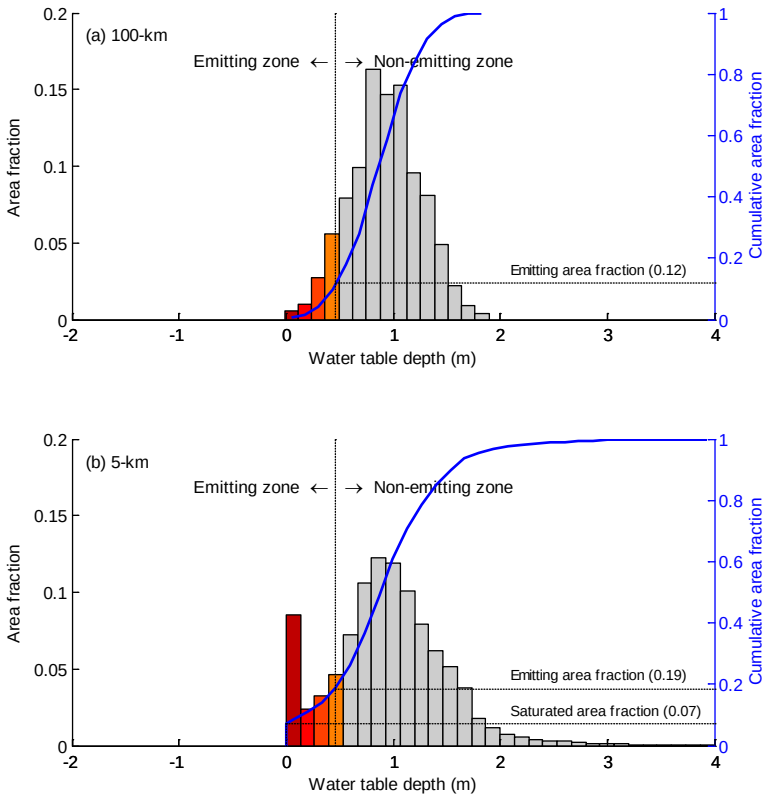

Fig. 4. Probability distributions of mean water table depth during the growing season (May–September) at 100 km **(a)** and 5 km **(b)** spatial resolutions across West Siberian Lowlands. The colored and grey bars indicate methane emitting and non-emitting zones, respectively; darker colored bars correspond to higher methane emitting rates.

BGD
10, 18455–18478, 2013

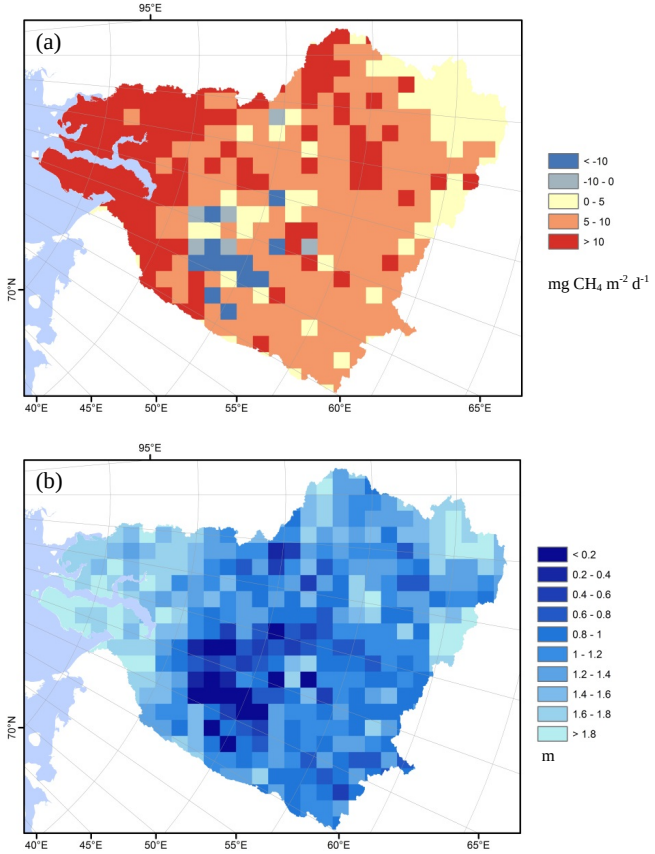

Fig. 5. The differences between mean 5 km methane fluxes and mean 100 km methane fluxes **(a)**, and mean water table depth **(b)**, during the growing season (May–September) across West Siberian Lowlands.

BGD
10, 18455–18478, 2013